Brief Communication

MOLECULAR METABOLISM

# ATGL-1 mediates the effect of dietary restriction and the insulin/IGF-1 signaling pathway on longevity in *C. elegans*

**Nava Zaarur, Kathleen Desevin, James Mackenzie, Avery Lord, Alla Grishok**, Konstantin V. Kandror***

## ABSTRACT

**Objective:** Animal lifespan is controlled through genetic pathways that are conserved from nematodes to humans. Lifespan-promoting conditions in nematodes include fasting and a reduction of insulin/IGF signaling. Here we aimed to investigate the input of the *Caenorhabditis elegans* homologue of the mammalian rate-limiting lipolytic enzyme Adipose Triglyceride Lipase, ATGL-1, in longevity control.

**Methods:** We used a combination of genetic and biochemical approaches to determine the role of ATGL-1 in accumulation of triglycerides and regulation of longevity.

**Results:** We found that expression of ATGL is increased in the insulin receptor homologue mutant *daf-2* in a FoxO/DAF-16-dependent manner. ATGL-1 is also up-regulated by fasting and in the *eat-2* loss-of-function mutant strain. Overexpression of ATGL-1 increases basal and maximal oxygen consumption rate and extends lifespan in *C. elegans*. Reduction of ATGL-1 function suppresses longevity of the long-lived mutants *eat-2* and *daf-2*.

**Conclusion:** Our results demonstrate that ATGL is required for extended lifespan downstream of both dietary restriction and reduced insulin/IGF signaling.



**Keywords** ATGL-1; Dietary restriction; DAF-2; DAF-16; Longevity; *C. elegans*

## 1. INTRODUCTION

In metazoans, the insulin/IGF1 signaling pathway (IIS) coordinates nutrient and energy availability with growth, metabolism, and longevity [1]. Two major "signaling nodes" [2], FoxO- and TORC1-centered, are responsible for the effect of nutrients and IIS on the lifespan [3–6]. Transcription factor FoxO1 (Forkhead box O 1) that adapts mammalian organisms to starvation is negatively regulated by IIS *via* Akt-mediated phosphorylation and nuclear exclusion [7,8]. At the same time, oligomeric Ser/Thr protein kinase TORC1 (Target Of Rapamycin Complex 1) is activated by Akt and nutrients and promotes anabolic processes while inhibiting catabolism [9].

The downstream target(s) of FoxO and TORC1 that transmit longevity signal(s) remain largely unknown. Given that both FoxO and TORC1 are ubiquitously expressed and regulate a plethora of important biological responses, identification of the specific pathway(s) that control longevity is challenging. In fact, we do not even know whether FoxO and mTORC1 are involved in the same pathway or mediate different pathways of the longevity control.

We have recently found that FoxO1 [10,11] and mTORC1 [12–14] control the rates of lipolysis in mammalian cells by regulating expression of adipose triglyceride lipase (ATGL; a.k.a. desnutrin, PNPLA2, TTS2.2, $iPLA_2\zeta$). Although complete hydrolysis of triglycerides (TG) to glycerol and fatty acids (FA) is performed jointly by tri- di- and monoacylglyceride lipases, ATGL represents the rate-limiting lipolytic enzyme. In other words, in every mammalian experimental system tested thus far, elevated ATGL expression increases, while attenuated ATGL expression decreases, both basal and cAMP-stimulated lipolysis [12,15–24].

Since known biochemical pathways that control longevity converge on the regulation of ATGL expression, we have hypothesized that ATGL may represent the long sought after target of the nutrient and insulin/IGF1 signaling pathways that regulate life span. Here, we utilize the nematode *C. elegans*, a well-characterized and widely used model for longevity studies, and show that expression of the *C. elegans* ATGL homologue ATGL-1 (C05D11.7) is controlled by nutrients and the DAF-2/DAF-16 pathway. Moreover, we find that the partial loss-of-function ATGL-1 mutant, ATGL-1 [P87S], blocks the life-extending effects of dietary restriction (in *eat-2* loss-of-function model) and DAF-2 deficiency, whereas over-expression of ATGL-1 increases *C. elegans* lifespan.

Department of Biochemistry, Boston University School of Medicine, Boston, MA, 02118, USA

*Corresponding author. Boston University School of Medicine, Department of Biochemistry, 72 East Concord St., Boston, MA, 02118, USA. E-mail: kkandror@bu.edu (K.V. Kandror).

**Corresponding author. Boston University School of Medicine, Department of Biochemistry, 72 East Concord St., Boston, MA, 02118, USA. E-mail: agrishok@bu.edu (A. Grishok).

Received May 20, 2019 • Revision received June 28, 2019 • Accepted July 2, 2019 • Available online 5 July 2019

https://doi.org/10.1016/j.molmet.2019.07.001

 

## 2. MATERIALS AND METHODS

### 2.1. *C. elegans* strains

All *C. elegans* strains were maintained at 20 °C using standard methods [25]. The wild-type strain used was the *C. elegans* Bristol strain N2. The following strains were obtained from the Caenorhabditis Genetics Center (CGC): GR1307 *daf-16(mgDf50) I*, CB1370 *daf-2(e1370) III*, HT1890 *daf-16(mgDf50) I*; *daf-2(e1370) III*, VS20 *hjls67 [atgl-1p::atgl-1::gfp + mec-7::rfp]*, and VC20458 containing *atgl-1 (gk176565) [P87S] III*. The *atgl-1(gk176565)* mutation was outcrossed four times to generate AGK785 *atgl-1(gk176565)*. The AVS518 *eat-2(ad465) II* strain was obtained from Dr. Andrew Samuelson (University of Rochester).

Other strains produced in this study include:

AGK786: atgl-1(gk176565) daf-2(e1370) III

AGK787: *eat-2(ad465) II*; *atgl-1(gk176565)*

AGK788: daf-2(e1370) III; hjls67

AGK789: daf-16(mgDf50) I; daf-2(e1370) III; hjls67

### 2.2. Fasting conditions

L1 larvae were synchronized by treatment of gravid adults with 20% alkaline hypochlorite and allowing embryos to hatch in the M9 buffer (0.3% $KH_2PO_4$, 0.6% $Na_2HPO_4$, 0.5% NaCl, 1 mM $MgSO_4$) overnight. Hatched worms were grown to the L4 stage on NGM plates, harvested, and washed four times with M9 buffer. The worms were then split into two groups that were grown for 6 h on NGM agar plates either seeded with *E. coli* OP50 (Fed) or without bacterial food (Fasted).

### 2.3. Measurement of triglyceride content

Synchronized L4 stage worms (3000–5000) were pelleted by microcentrifugation at 13,000 rpm for 10 min, re-suspended in 50 μl of 5% Triton X-100 supplied with the protease inhibitor cocktail (Sigma, St. Louis, MO), and sonicated by 3 cycles (10 s each) using a Sonic Dismembrator (Fisher Scientific, Waltham, MA) set at power output "3" at 4 °C. Protein concentration in lysates was determined using the Pierce BCA Protein Assay kit (Fisher Scientific) on a Biotek Synergy™ HT microplate reader (Biotek, Winooski, Vermont). The lysates underwent two cycles of heating to 90 °C for 5 min, each followed by vortexing, cooling to room temperature, and centrifugation at 8000 $\times g$ for 5 min. Triglycerides were measured using Triglyceride Quantification kit (Biovision, Milpitas, CA) according to the manufacturer's protocol.

### 2.4. Oil-Red-O staining

Synchronized L4 stage worms were harvested, washed with PBS, and fixed in 1 ml of methanol at −20 °C for 5 min. Then, 2 ml of PBST (PBS with 0.01% Tween-20) was added, and worms were pelleted by centrifugation at 1000 rpm for 1 min. Supernatant was removed, and worms were washed twice with PBST in the same regime. Water (60% by volume) was added to Oil Red O (0.5% solution in isopropanol, Sigma) at room temperature, and, in 10 min, the solution was filtered through a 0.4 μm syringe filter. Fixed worms were stained with filtered 40% isopropanol Oil Red O solution (1 ml) for 20 min, washed twice with PBST, and mounted on slides with 3% agar. Images were taken using an inverted epi-fluorescent microscope (Carl Zeiss; Axio Observer D1) with a color camera.

### 2.5. RT-qPCR

Synchronized L4 stage worms (1000–2000) were washed with PBS, re-suspended in 1 ml of cold TRIzol (Ambion, Austin, TX), incubated at −80 °C for at least 1 h, and RNA was isolated according to the manufacturer's instructions. Reverse transcription (RT) was carried out using a RETROscript kit (Ambion), and quantitative RT-PCR was performed using iTag Universal SYBR Green Supermix (Bio-Rad, Hercules, CA) according to the protocol of manufacturer with the following primers. *atgl-1*: forward 5′ GATCGACCGATGATTTATCGAG 3′, reverse 5′ GAGCCAATCCACATTTGGTC 3'; *actin-1/3*: forward, 5′ CACGAGACTTCTTACAACTCC 3′, reverse, 5′GCATACGATCAGCAATTCCT 3'. Relative expression levels of all mRNAs were normalized to *actin-1/3* mRNA.

### 2.6. Measurement of oxygen consumption rates

OCR was measured by XF96 Extracellular Flux Analyzer - Seahorse (Agilent, Santa Clara, CA) using Seahorse's cartridges and plates (Bioscience). All measurements have been done at 28 °C. Synchronized worms (L3-L4 stage) were washed 3 times with M9 buffer, and ca. 20 worms were placed in a well with 200 μL M9 buffer. For each strain, 10 wells were used. Basal OCR was measured every 5 min. After that, carbonyl cyanide 4-(trifluoromethoxy) phenylhydrazone (FCCP, Sigma) was injected to each well to the final concentration of 10 μM, and maximal OCR was measured every 5 min. Finally, sodium azide (Sigma) was injected to the final concentration of 40 mM and non-mitochondrial OCR was measured every 5 min. After all measurements, worms in each well were re-counted, and results were normalized by their exact number.

### 2.7. Longevity experiments

Young adult worms were allowed to lay eggs for 6 h and then manually removed from the plates. The hatched L1 larvae were plated on ten 6 cm NGM Petri dishes, ca. twenty larvae per plate, and their lifespan was monitored every day. During the gravid adult stage, adult worms were separated from eggs/L1 larva and moved to new plates. The hatching day was considered Day 1. Death was scored if the animal did not move after repeated prodding with a pick. Animals disappearing from the plate or dying due to bursting or internal larva hatching were excluded from scoring, but included in the statistical analysis. Statistical significance ($p$ value) of lifespan differences between the strains was determined by log-rank analysis for a single comparison and log-rank with Bonferroni correction for multiple comparisons using Oasis-2 software [26]. Time point when 50% of the worm population stays alive was considered mean lifespan. Each lifespan experiment was repeated three times with each group of worms. Combined $p$ value was calculated by the Fisher's combined probability test. Representative life span experiments are shown in the Figures, and all repeats are listed in Table 1.

### 2.8. Fluorescence microscopy

Live animals were mounted on 2% agarose pads and immobilized with sodium azide. Images were taken either using Axiovert 200 or Zeiss AxioImager Z1 (Carl Zeiss, Germany) with a 20X objective. Identical exposure times were used when GFP intensity was compared between different conditions. ImageJ software was used to assess the level of fluorescence.

## 3. RESULTS

### 3.1. ATGL-1 increases oxygen consumption and longevity

Fasting of wild type (N2) worms for 6 h depletes their TG reserves (Figure 1A (top) & B (left)) and up-regulates the *atgl-1* mRNA (Figure 1C). To analyze expression of the ATGL-1 protein, we have utilized the VS20 strain that contains chromosome-integrated transgenic array *hjls67 [atgl-1p::atgl-1::GFP + mec-7p::RFP]* [27] (that will

 

**Table 1** — Mean lifespans of *C. elegans* strains.

| Figure | Individual Experiments | Genotypes Compared | # of Worms | Mean Lifespan ± SEM (days) | % Lifespan Change compared to N2 or as noted | p Value | Combined p Value compared to N2 or as noted |
|---|---|---|---|---|---|---|---|
| 1H | 1 | N2 | 206 | 14.07 ± 0.35 | | | |
| | | *atgl-1::gfp* | 202 | 18.62 ± 0.44 | +32.3 | <1.0e-10 | |
| | 2 | N2 | 132 | 15.74 ± 0.44 | | | |
| | | *atgl-1::gfp* | 82 | 20.20 ± 0.78 | +28.3 | 7.8e-8 | |
| | 3 | N2 | 90 | 14.78 ± 0.39 | | | |
| | | *atgl-1::gfp* | 112 | 20.87 ± 0.67 | +41.2 | <1.0e-10 | <1.0e-4 |
| 2F | 1 | N2 | 146 | 13.90 ± 0.35 | | | |
| | | *eat-2(ad453)* | 104 | 18.81 ± 0.80 | +35.3 | 1.0e-3 | |
| | | *atgl-1(P87S)* | 156 | 13.8 ± 0.30 | −0.7 | 0.5495 | |
| | | *eat-2(ad453); atgl-1(P87S)* | 166 | 12.58 ± 0.18 | −9.5<br>−33.1 (comp. to *eat-2*) | 1.0e-3<br><1.0e-10 (comp. to *eat-2*) | |
| | 2 | N2 | 216 | 13.20 ± 0.33 | | | |
| | | *eat-2(ad453)* | 187 | 18.77 ± 0.45 | +42.2 | <1.0e-10 | |
| | | *atgl-1(P87S)* | 180 | 14.26 ± 0.24 | −8.0 | 0.0326 | |
| | | *eat-2(ad453); atgl-1(P87S)* | 206 | 12.58 ± 0.28 | −4.7<br>−33.0 (comp. to *eat-2*) | 0.7903<br><1.0e-10 (comp. to *eat-2*) | |
| | 3 | N2 | 217 | 13.3 ± 0.34 | | | |
| | | *eat-2(ad453)* | 202 | 20.33 ± 0.51 | +52.9 | <1.0e-10 | <1.0e-4 |
| | | *atgl-1(P87S)* | 255 | 12.52 ± 0.17 | −5.9 | 0.85 | 0.21 |
| | | *eat-2(ad453); atgl-1(P87S)* | 251 | 15.43 ± 0.41 | +16.0<br>−24.1 (comp. to *eat-2*) | 4.3e-6<br><1.0e-10 (comp. to *eat-2*) | <1.0e-4 (comp. to *eat-2*) |
| 3D | 1 | N2 | 100 | 12.0 ± 0.39 | | | |
| | | *daf-2(e1370)* | 90 | 27.73 ± 1.7 | +131.1 | <1.0e-10 | |
| | | *atgl-1(P87S)* | 102 | 10.92 ± 0.30 | −9.0 | 0.1268 | |
| | | *daf-2(e1370); atgl-1(P87S)* | 110 | 14.90 ± 0.89 | +24.2<br>−46.3 (comp. to *daf-2*) | 3.3e-3<br><1.0e-10 (comp. to *daf-2*) | |
| | 2 | N2 | 189 | 14.46 ± 0.29 | | | |
| | | *daf-2(e1370)* | 171 | 28.22 ± 0.81 | +95.2 | <1.0e-10 | |
| | | *atgl-1(P87S)* | 174 | 14.16 ± 0.30 | −2.1 | 1 | |
| | | *daf-2(e1370); atgl-1(P87S)* | 155 | 16.87 ± 0.63 | +16.7<br>−40.2 (comp. to *daf-2*) | 3.0e-4<br><1.0e-10 (comp. to *daf-2*) | |
| | 3 | N2 | 194 | 14.07 ± 0.35 | | | |
| | | *daf-2(e1370)* | 113 | 29.99 ± 1.65 | +113.1 | <1.0e-10 | <1.0e-4 |
| | | *atgl-1(P87S)* | 180 | 14.26 ± 0.24 | +1.4 | 1 | 0.66 |
| | | *daf-2(e1370); atgl-1(P87S)* | 134 | 16.84 ± 0.63 | +19.7<br>−43.8 (comp. to *daf-2*) | 4.1e-3<br><1.0e-10 (comp. to *daf-2*) | <1.0e-4<br><1.0e-4 (comp. to *daf-2*) |

be further referred to as *atgl-1::gfp*). As shown in Figure 1D,E, fasting increases ATGL-1 protein levels. Also, overexpression of *atgl-1::gfp* decreases TG reserves in both fed and, to a lesser extent, fasted worms (Figure 1A bottom & 1B right). In agreement with these results, it has been shown previously that down-regulation of *atgl-1* by RNAi prevents TG depletion in adult worms subjected to fasting [28].

In mammals, ATGL-mediated lipolysis produces endogenous ligands for PPARα, its isotype PPARδ, and co-activator PGC-1α to control mitochondrial biogenesis and functions [29–34]. In agreement with these results, we have found that overexpression of *atgl-1::gfp* increases both basal and maximal oxygen consumption rate as well as reserve respiratory capacity (Figure 1F,G). As healthy mitochondria are essential for longevity in both mammals [35] and *C. elegans* [36], we decided to determine the effect of *atgl-1::gfp* on longevity. Interestingly, the life span of the VS20 strain is significantly longer compared to that of N2 (Figure 1H and Table 1).

The latter result may seem to contradict a reported negative effect of ATGL-1 on the lifespan of *aak-2* (the *C. elegans* AMP-activated kinase α2 catalytic subunit) mutant dauer larvae [37]. However, dauer represents an arrested dormant state that nematodes convert to in the absence of food. Dauer larvae do not feed and rely on stored energy for their survival. Therefore, in this case, the lipolytic activity of ATGL-1 appears to be suppressed by AMPK, and ATGL-1 de-repression in *aak-2* mutant worms leads to faster depletion of nutrient stores and lifespan reduction.

### 3.2. Reduction of ATGL-1 function suppresses longevity of the *eat-2* loss-of-function mutant strain

As deletion of the *atgl-1* gene (the *tm3116* allele) is lethal [38], we used a partial loss-of-function *atgl-1* mutant for further experiments. To obtain a viable *atgl-1* mutant allele we searched a list of strains generated by the Million Mutation Project [39] and identified *atgl-1(gk176565 [P87S])* as a potential candidate. We reasoned that substitution of a proline by a serine in the extended conserved catalytic domain of ATGL [40] should impact ATGL function, through reducing ATGL catalytic activity and/or protein stability. Importantly, this mutation did not change levels of the *atgl*-1 mRNA (not shown). The *atgl-1(gk176565)* allele was outcrossed four times prior to its use in experiments described below.

In agreement with our expectations, the *atgl-1(P87S)* mutant accumulated significantly more TG than N2. Furthermore, fasting of the *atgl-1(P87S)* strain does not decrease its TG reserves (Figure 2A,B), which supports our hypothesis that P87S is a reduction-of-function ATGL-1 mutation.

To test whether or not ATGL-1 mediates the effect of fasting on longevity, we took advantage of a long lived strain *eat-2(ad465)* that

 

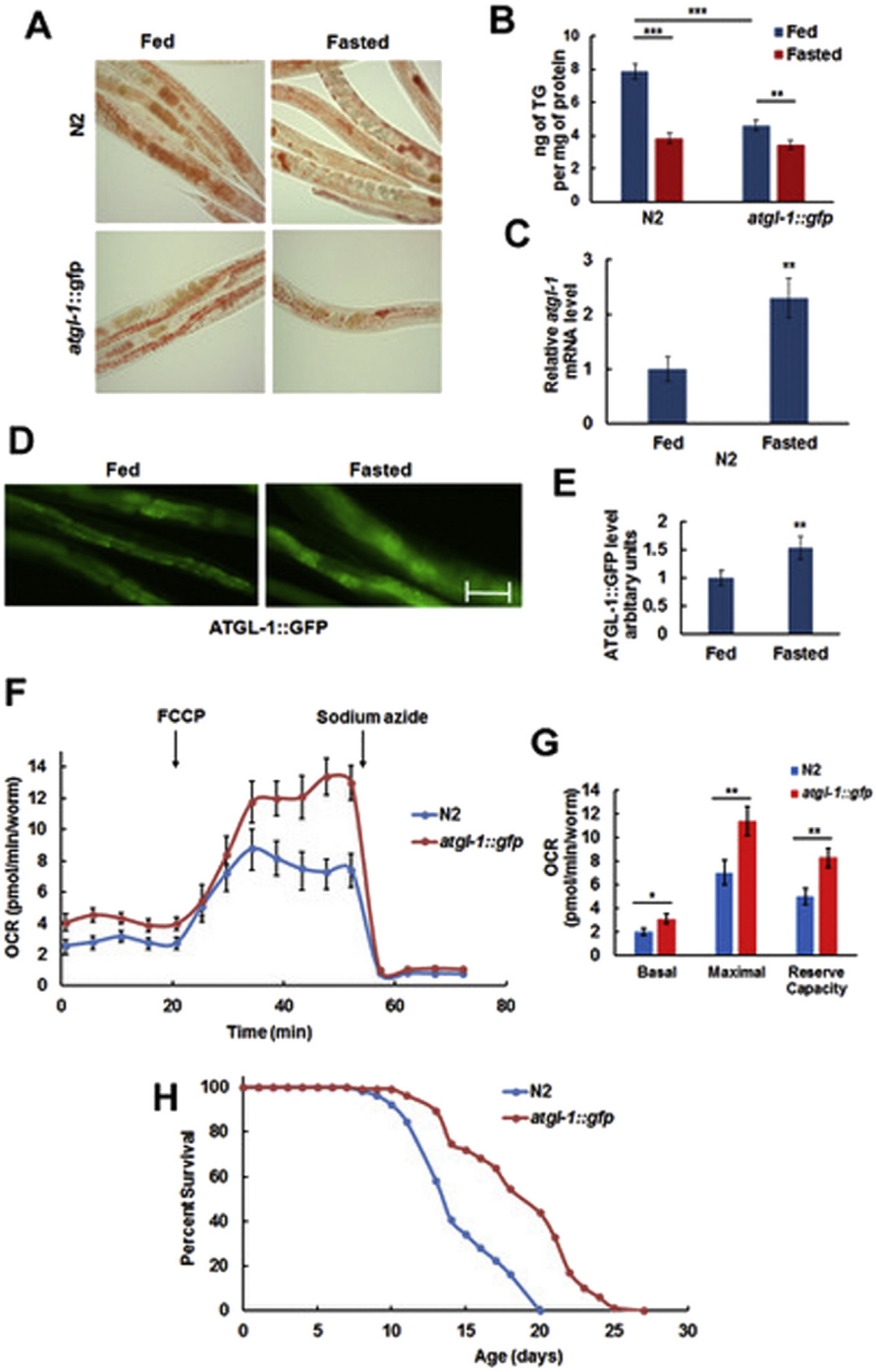


**Figure 1: ATGL-1 is up-regulated by fasting and increases oxygen consumption rate as well as longevity of *C. elegans*.** (A) Wild type (N2) and *atgl-1::gfp* worms were split into control (Fed) and Fasted groups and stained with Oil Red O. (B) Triglyceride content was measured in Fed and Fasted groups of N2 and *atgl-1::gfp* worms. (C) RNA was extracted from Fed and Fasted groups, and *atgl-1* mRNA levels were measured by qRT-PCR; *actin-1/3* was used for normalization. (D) Fed and Fasted L4 stage *atgl-1::gfp* worms were visualized by fluorescence microscopy (200X, equal exposure times). Bar — 50 μM. (E) Quantification of the results shown in panel D by ImageJ (10 randomly selected worms per group). (F) Oxygen Consumption Rate (OCR) of N2 and *atgl-1::gfp* L4 worms was measured by XF96 Extracellular Flux Analyzer Seahorse, as described in Experimental Procedures. Each experiment was performed with ca. 200 worms and repeated 3 times. (G) Average basal OCR was calculated as the mean of the first five measurements after subtraction of average non-mitochondrial OCR; average maximal OCR is the mean of the last (before addition of sodium azide) five measurements after subtraction of average non-mitochondrial OCR; reserve respiratory capacity is the difference between average maximal and basal OCR. (H) The lifespan of *atgl-1::gfp* worms is extended by 32% in comparison to N2 ($p$ value $<$ 1.0e-10, log-rank analysis). Panels B, C, E-G show an average result of three independent experiments ±SEM, $p$ values were calculated by unpaired two-tailed $t$-test. *$p < 0.05$; **$p < 0.01$; ***$p < 0.001$.

mimics several aspects of dietary restriction due to the defect in pharyngeal function hence insufficient food uptake [41]. As expected, *eat-2* mutant worms accumulated less TG than N2 (Figure 2C,D). Interestingly, the levels of *atgl*-1 mRNA in fed *eat-2(ad465)* worms were twice as high as in fed N2 strain (Figure 2E), and similar to the fasted N2 (Figure 1C). We then combined *atgl-1(P87S)* with *eat-*

 

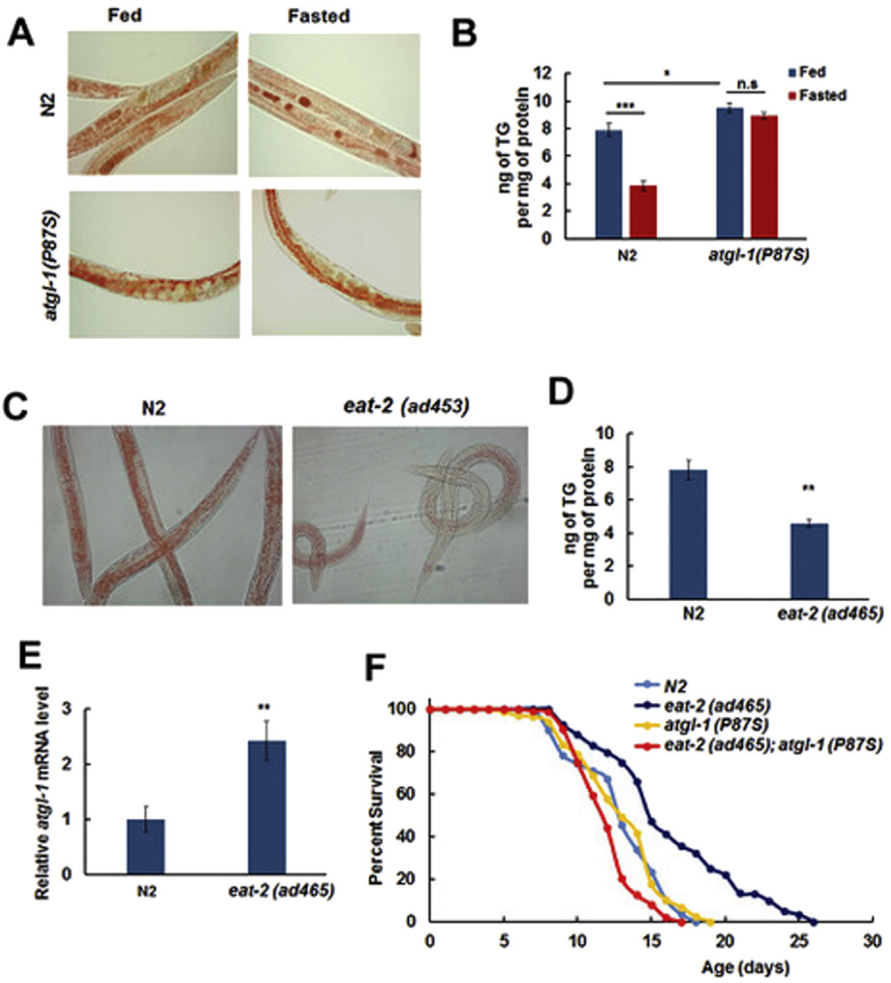


**Figure 2: Increased longevity of the *eat-2(ad465)* strain is suppressed by *atgl-1(P87S)*.** (A) N2 and *atgl-1(P87S)* worms were split into Fed and Fasted groups and stained with Oil Red O. (B) Triglyceride content was measured in Fed and Fasted groups of N2 and *atgl-1(P87S)* worms. (C) N2 and *eat-2(ad465)* worms were stained with Oil Red O. (D) Triglyceride content was measured in N2 and *eat-2(ad465)* worms. (E) RNA was extracted from N2 and *eat-2(ad465)* worms, and *atgl-1* mRNA levels were measured by qRT-PCR; *actin-1/3* was used for normalization. (F) The lifespan of *eat-2(ad465)* worms is extended by 35.3% in comparison to N2 ($p$ value 1.0e-3, log-rank with Boneferroni correction), while the lifespan of *eat-2(ad465); atgl-1(P97S)* worms is decreased by 33.1% in comparison to *eat-2(ad465)* ($p$ value $<$ 1.0e-10, log-rank with Bonferroni correction). Panels B, D, and E show an average result of three independent experiments $\pm$SEM, $p$ values were calculated by unpaired two-tailed $t$-test. *$p<$ 0.05; **$p <$ 0.01; ***$p <$ 0.001.

*2(ad465)* to obtain the *eat-2(ad465); atgl-1(P87S)* double mutant strain and used it in longevity experiments along with N2, *atgl-1(P87S)*, and *eat-2(ad465)*. As shown in Figure 2F and Table 1, *atgl-1(P87S)* completely suppressed the extended life span of *eat-2(ad465)*. Therefore, ATGL-1 is required for the life span extension in this model of dietary restriction.

### 3.3. ATGL-1 is regulated by the DAF-2/DAF-16 axis and is required for extended lifespan of *daf-2* mutants

In mammalian adipocytes, expression of ATGL is suppressed by insulin *via* inhibition of FoxO1 [11]. The worm expresses homologues of the insulin receptor (DAF-2) and FoxO (DAF-16), but it is unknown whether expression of ATGL-1 in *C. elegans* is controlled by DAF-2 and DAF-16. Supporting this possibility, bioinformatics analysis shows a canonical DAF-16 binding site in the promoter of the *atgl-1* gene (not shown). Therefore, we generated *daf-2(e1370)* and *daf-2(e1370); daf-16(mgDf50)* strains containing the *atgl-1::gfp* translational fusion reporter. Indeed, we observed elevated ATGL-1::GFP protein (Figure 3A,B) and *atgl*-1 mRNA (Figure 3C) expression in *daf-2(e1370)* compared to the background transgenic strain. Importantly, this effect was suppressed by the *daf-16(mgDf50)* null allele (Figure 3A—C). These results confirm the evolutionary conservation of ATGL regulation *via* the insulin receptor/FoxO1 axis from *C. elegans* to mammals.

To determine whether or not increased life span of the *daf-2(e1370)* mutant was dependent on *atgl-1*, we have crossed it with the *atgl-1(P87S)* strain. Our longevity experiments demonstrate that the life span of *daf-2(e1370); atgl-1(P87S)* was significantly (by ca. 46%) shorter compared to that of *daf-2(e1370)* alone (Figure 3D and Table 1). Therefore, ATGL-1 function is required downstream of both dietary restriction (Figure 2F) and DAF-16/FoxO pathways to extend life.

## 4. DISCUSSION

Wang et al. [42] have previously identified another "life extending" lipase, LIPL-4 (*K04A8.5*) that shares a high degree of homology with mammalian lysosomal acid lipase and, therefore, is likely to be localized in lysosomes. Similar to cytosolic ATGL-1, LIPL-4 increases

 

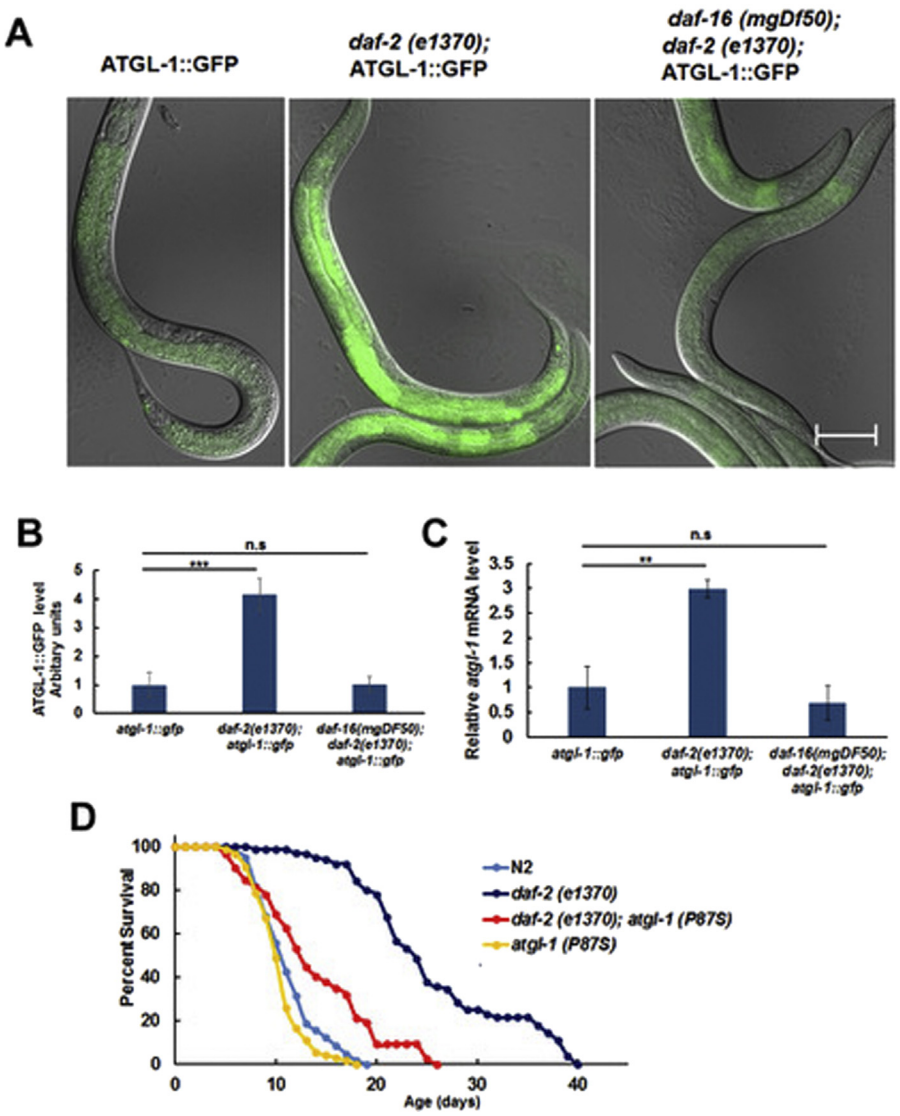


**Figure 3: Expression of ATGL-1 is regulated by the *daf-2/daf-16* pathway, and *atgl-1(P87S)* suppresses longevity of the *daf-2* mutant.** (A) L4 stage worms were visualized by fluorescence microscopy (200X, equal exposure times). Bar — 50 μM. (B) Quantification of the results shown in panel A by ImageJ (10 randomly selected worms per group). (C) Expression of the *atgl-1* mRNA was measured by RT-qPCR; *actin-1/3* was used for normalization. (D) The lifespan of *daf-2(e1370)* worms is increased by 131.1% in comparison to N2 ($p$ value $<$ 1.0e-10, log-rank with Boneferroni correction), while the lifespan of *daf-2(e1370); atgl-1(P97S)* worms is decreased by 46.3% in comparison to *daf-2(e1370)* ($p$ value $<$ 1.0e-10, log-rank with Boneferroni correction). Panel D shows an average result of three independent experiments ±SEM, $p$ values were calculated by unpaired two-tailed $t$-test. $^{**}p < 0.01$; $^{***}p < 0.001$, n.s. — not significant.

mitochondrial oxidation and reduces lipid storage [43]. In *C. elegans*, expression of both LIPL-4 [42] and ATGL-1 (this report) is activated by DAF-16; in mammalian cells, lysosomal acid lipase and ATGL are also co-regulated by FoxO1 [44]. Thus, both lysosomal and cytoplasmic lipases are regulated by the same evolutionary conserved signaling pathway and are essential for the life span control in *C. elegans*.

Adipose tissue plays a very special role in the control of the life span in mammals [45]. In particular, caloric restriction decreases TG stores in adipocytes and increases longevity, while obesity has the opposite effect [46]. Genetic ablation of the insulin receptor specifically in adipose tissue suppresses TG accumulation and significantly extends life span in mice [47]. Knock out of IRS-1 produces a similar outcome [48]. As regulatory pathways of ATGL expression are conserved from yeast [14] through *C. elegans* (this report) and *Drosophila* [49] to mammals [11,14], it is feasible that ATGL may have a systemic life extending effect in higher eukaryotes.

## 5. CONCLUSIONS

Our results suggest that (a) evolutionary conserved dietary restriction and the IIS pathways converge on ATGL-1 expression, and (b) ATGL-1 is required for the extension of life span in response to dietary restriction and reduced IIS.

## ACKNOWLEDGEMENTS

This work was supported by research grants from the NIH DK52057 & DK107498 to K.V.K., the research grant from the American Diabetes Association 1-18-IBS-266 to

 

K.V.K., the BU-CTSI Pilot Award 1UL1TR001430 to K.V.K. and A.G., and by Boston Obesity Nutrition Research Center supported by P30DK046200 to Dr. Corkey. Strains used in this study were obtained from the Caenorhabditis Genetics Center, which is funded by NIH Office of Research Infrastructure Programs (P40 OD010440). The VC20458 strain was provided by the *C. elegans* Reverse Genetics Core Facility at the University of British Columbia, which is part of the International *C. elegans* Gene Knockout Consortium. We thank Dr. Andrew Samuelson (University of Rochester) for sharing the AVS518 *eat-2(ad465) II* strain.

## CONFLICT OF INTEREST

None.

## REFERENCES

[1] Templeman, N.M., Murphy, C.T., 2018. Regulation of reproduction and longevity by nutrient-sensing pathways. The Journal of Cell Biology 217(1): 93–106.

[2] Taniguchi, C.M., Emanuelli, B., Kahn, C.R., 2006. Critical nodes in signalling pathways: insights into insulin action. Nature Reviews Molecular Cell Biology 7(2):85–96.

[3] Riera, C.E., Dillin, A., 2015. Tipping the metabolic scales towards increased longevity in mammals. Nature Cell Biology 17(3):196–203.

[4] Kenyon, C.J., 2010. The genetics of ageing. Nature 464(7288):504–512.

[5] Johnson, S.C., Rabinovitch, P.S., Kaeberlein, M., 2013. mTOR is a key modulator of ageing and age-related disease. Nature 493(7432):338–345.

[6] Singh, P.P., Demmitt, B.A., Nath, R.D., Brunet, A., 2019. The genetics of aging: a vertebrate perspective. Cell 177(1):200–220.

[7] Calnan, D.R., Brunet, A., 2008. The FoxO code. Oncogene 27(16):2276–2288.

[8] Gross, D.N., van den Heuvel, A.P., Birnbaum, M.J., 2008. The role of FoxO in the regulation of metabolism. Oncogene 27(16):2320–2336.

[9] Saxton, R.A., Sabatini, D.M., 2017. mTOR signaling in growth, metabolism, and disease. Cell 168(6):960–976.

[10] Chakrabarti, P., English, T., Karki, S., Qiang, L., Tao, R., Kim, J., et al., 2011. SIRT1 controls lipolysis in adipocytes via FOXO1-mediated expression of ATGL. The Journal of Lipid Research 52(9):1693–1701.

[11] Chakrabarti, P., Kandror, K.V., 2009. FoxO1 controls insulin-dependent adipose triglyceride lipase (ATGL) expression and lipolysis in adipocytes. Journal of Biological Chemistry 284(20):13296–13300.

[12] Chakrabarti, P., English, T., Shi, J., Smas, C.M., Kandror, K.V., 2010. Mammalian target of rapamycin complex 1 suppresses lipolysis, stimulates lipogenesis, and promotes fat storage. Diabetes 59(4):775–781.

[13] Chakrabarti, P., Kandror, K.V., 2015. The role of mTOR in lipid homeostasis and diabetes progression. Current Opinion in Endocrinology Diabetes and Obesity 22(5):340–346.

[14] Chakrabarti, P., Kim, J.Y., Singh, M., Shin, Y.K., Kim, J., Kumbrink, J., et al., 2013. Insulin inhibits lipolysis in adipocytes via the evolutionarily conserved mTORC1-Egr1-ATGL-mediated pathway. Molecular and Cellular Biology 33(18):3659–3666.

[15] Smirnova, E., Goldberg, E.B., Makarova, K.S., Lin, L., Brown, W.J., Jackson, C.L., 2006. ATGL has a key role in lipid droplet/adiposome degradation in mammalian cells. EMBO Reports 7(1):106–113.

[16] Zimmermann, R., Strauss, J.G., Haemmerle, G., Schoiswohl, G., Birner-Gruenberger, R., Riederer, M., et al., 2004. Fat mobilization in adipose tissue is promoted by adipose triglyceride lipase. Science 306(5700):1383–1386.

[17] Villena, J.A., Roy, S., Sarkadi-Nagy, E., Kim, K.H., Sul, H.S., 2004. Desnutrin, an adipocyte gene encoding a novel patatin domain-containing protein, is induced by fasting and glucocorticoids: ectopic expression of desnutrin increases triglyceride hydrolysis. Journal of Biological Chemistry 279(45): 47066–47075.

[18] Jenkins, C.M., Mancuso, D.J., Yan, W., Sims, H.F., Gibson, B., Gross, R.W., 2004. Identification, cloning, expression, and purification of three novel human calcium-independent phospholipase A2 family members possessing triacylglycerol lipase and acylglycerol transacylase activities. Journal of Biological Chemistry 279(47):48968–48975.

[19] Haemmerle, G., Lass, A., Zimmermann, R., Gorkiewicz, G., Meyer, C., Rozman, J., et al., 2006. Defective lipolysis and altered energy metabolism in mice lacking adipose triglyceride lipase. Science 312(5774):734–737.

[20] Bezaire, V., Mairal, A., Ribet, C., Lefort, C., Girousse, A., Jocken, J., et al., 2009. Contribution of adipose triglyceride lipase and hormone-sensitive lipase to lipolysis in hMADS adipocytes. Journal of Biological Chemistry 284(27): 18282–18291.

[21] Miyoshi, H., Perfield 2nd, J.W., Obin, M.S., Greenberg, A.S., 2008. Adipose triglyceride lipase regulates basal lipolysis and lipid droplet size in adipocytes. Journal of Cellular Biochemistry 105(6):1430–1436.

[22] Kershaw, E.E., Hamm, J.K., Verhagen, L.A., Peroni, O., Katic, M., Flier, J.S., 2006. Adipose triglyceride lipase: function, regulation by insulin, and comparison with adiponutrin. Diabetes 55(1):148–157.

[23] Gronke, S., Mildner, A., Fellert, S., Tennagels, N., Petry, S., Muller, G., et al., 2005. Brummer lipase is an evolutionary conserved fat storage regulator in Drosophila. Cell Metabolism 1(5):323–330.

[24] Kurat, C.F., Natter, K., Petschnigg, J., Wolinski, H., Scheuringer, K., Scholz, H., et al., 2006. Obese yeast: triglyceride lipolysis is functionally conserved from mammals to yeast. Journal of Biological Chemistry 281(1):491–500.

[25] Brenner, S., 1974. The genetics of Caenorhabditis elegans. Genetics 77(1): 71–94.

[26] Han, S.K., Lee, D., Lee, H., Kim, D., Son, H.G., Yang, J.S., et al., 2016. OASIS 2: online application for survival analysis 2 with features for the analysis of maximal lifespan and healthspan in aging research. Oncotarget 7(35):56147–56152.

[27] Zhang, S.O., Box, A.C., Xu, N., Le Men, J., Yu, J., Guo, F., et al., 2010. Genetic and dietary regulation of lipid droplet expansion in Caenorhabditis elegans. Proceedings of the National Academy of Sciences of the United States of America 107(10):4640–4645.

[28] Lee, J.H., Kong, J., Jang, J.Y., Han, J.S., Ji, Y., Lee, J., et al., 2014. Lipid droplet protein LID-1 mediates ATGL-1-dependent lipolysis during fasting in Caenorhabditis elegans. Molecular and Cellular Biology 34(22): 4165–4176.

[29] Haemmerle, G., Moustafa, T., Woelkart, G., Buttner, S., Schmidt, A., van de Weijer, T., et al., 2011. ATGL-mediated fat catabolism regulates cardiac mitochondrial function via PPAR-alpha and PGC-1. Nature Medicine 17(9): 1076–1085.

[30] Khan, S.A., Sathyanarayan, A., Mashek, M.T., Ong, K.T., Wollaston-Hayden, E.E., Mashek, D.G., 2015. ATGL-catalyzed lipolysis regulates SIRT1 to control PGC-1alpha/PPAR-alpha signaling. Diabetes 64(2):418–426.

[31] Mottillo, E.P., Bloch, A.E., Leff, T., Granneman, J.G., 2012. Lipolytic products activate peroxisome proliferator-activated receptor (PPAR) alpha and delta in brown adipocytes to match fatty acid oxidation with supply. Journal of Biological Chemistry 287(30):25038–25048.

[32] Tang, T., Abbott, M.J., Ahmadian, M., Lopes, A.B., Wang, Y., Sul, H.S., 2013. Desnutrin/ATGL activates PPARdelta to promote mitochondrial function for insulin secretion in islet beta cells. Cell Metabolism 18(6):883–895.

[33] Biswas, D., Ghosh, M., Kumar, S., Chakrabarti, P., 2016. PPARalpha-ATGL pathway improves muscle mitochondrial metabolism: implication in aging. The FASEB Journal 30(11):3822–3834.

[34] Schreiber, R., Diwoky, C., Schoiswohl, G., Feiler, U., Wongsiriroj, N., Abdellatif, M., et al., 2017. Cold-Induced thermogenesis depends on ATGL-mediated lipolysis in cardiac muscle, but not Brown adipose tissue. Cell Metabolism 26(5):753–763 e757.

[35] Kauppila, T.E.S., Kauppila, J.H.K., Larsson, N.G., 2017. Mammalian mitochondria and aging: an update. Cell Metabolism 25(1):57–71.

 

[36] Chaudhari, S.N., Kipreos, E.T., 2018. The energy maintenance theory of aging: maintaining energy metabolism to allow longevity. Bioessays e1800005.
[37] Narbonne, P., Roy, R., 2009. Caenorhabditis elegans dauers need LKB1/AMPK to ration lipid reserves and ensure long-term survival. Nature 457(7226):210–214.
[38] Consortium, C.E.D.M., 2012. large-scale screening for targeted knockouts in the Caenorhabditis elegans genome. G3 (Bethesda) 2(11):1415–1425.
[39] Thompson, O., Edgley, M., Strasbourger, P., Flibotte, S., Ewing, B., Adair, R., et al., 2013. The million mutation project: a new approach to genetics in Caenorhabditis elegans. Genome Research 23(10):1749–1762.
[40] Cornaciu, I., Boeszoermenyi, A., Lindermuth, H., Nagy, H.M., Cerk, I.K., Ebner, C., et al., 2011. The minimal domain of adipose triglyceride lipase (ATGL) ranges until leucine 254 and can be activated and inhibited by CGI-58 and G0S2, respectively. PLoS One 6(10):e26349.
[41] Lakowski, B., Hekimi, S., 1998. The genetics of caloric restriction in Caenorhabditis elegans. Proceedings of the National Academy of Sciences of the United States of America 95(22):13091–13096.
[42] Wang, M.C., O'Rourke, E.J., Ruvkun, G., 2008. Fat metabolism links germline stem cells and longevity in *C. elegans*. Science 322(5903):957–960.
[43] Ramachandran, P.V., Savini, M., Folick, A.K., Hu, K., Masand, R., Graham, B.H., et al., 2019. Lysosomal signaling promotes longevity by adjusting mitochondrial activity. Developmental Cell 48(5):685–696 e685.
[44] Barbato, D.L., Aquilano, K., Ciriolo, M.R., 2014. FoxO1 at the nexus between fat catabolism and longevity pathways. Biochimica et Biophysica Acta Molecular and Cell Biology of Lipids 1841(10):1555–1560.
[45] Picard, F., Guarente, L., 2005. Molecular links between aging and adipose tissue. International Journal of Obesity (London) 29(Suppl. 1):S36–S39.
[46] Tchkonia, T., Morbeck, D.E., Von Zglinicki, T., Van Deursen, J., Lustgarten, J., Scrable, H., et al., 2010. Fat tissue, aging, and cellular senescence. Aging Cell 9(5):667–684.
[47] Bluher, M., Kahn, B.B., Kahn, C.R., 2003. Extended longevity in mice lacking the insulin receptor in adipose tissue. Science 299(5606):572–574.
[48] Selman, C., Lingard, S., Choudhury, A.I., Batterham, R.L., Claret, M., Clements, M., et al., 2008. Evidence for lifespan extension and delayed age-related biomarkers in insulin receptor substrate 1 null mice. The FASEB Journal 22(3):807–818.
[49] Birse, R.T., Choi, J., Reardon, K., Rodriguez, J., Graham, S., Diop, S., et al., 2010. High-fat-diet-induced obesity and heart dysfunction are regulated by the TOR pathway in Drosophila. Cell Metabolism 12(5):533–544.

 